

## Supporting Information

### Mandelic Acid Appended Chiral Gels as Efficient Templates for Multicolour Circularly Polarized Luminescence

Kumbam Lingeshwar Reddy,<sup>a†</sup> Jikson P. Mathew,<sup>a†</sup> Sonia Maniappan,<sup>a</sup> Catherine Tom,<sup>b</sup>  
Elizabeth Shiby,<sup>a</sup> Ravi Kumar Pujala,<sup>b</sup> Jatish Kumar<sup>a\*</sup>

<sup>a</sup>Department of Chemistry, Indian Institute of Science Education and Research (IISER) Tirupati,  
Tirupati, Andhra Pradesh-517507, India.

<sup>b</sup>Department of Physics, Indian Institute of Science Education and Research (IISER) Tirupati,  
Tirupati, Andhra Pradesh-517507, India.

Email: [jatish@iisertirupati.ac.in](mailto:jatish@iisertirupati.ac.in)

Page No.	Contents
S3 – S6	Experimental section
S4	Fig. S1. Scheme illustrating the synthesis of compound <b>2</b> .
S7	Fig. S2. <sup>1</sup> H NMR spectra of compound <b>1</b> .
S8	Fig. S3. <sup>13</sup> C NMR spectra of compound <b>1</b> .
S9	Fig. S4. HRMS data of compound <b>1</b> .
S9	Fig. S5. UV-visible spectra of <b>1R</b> in ethanol.
S10	Table S1. Behaviour of MA-based gelator in different solvent systems.
S11	Fig. S6. NMR titration plot of compound <b>1</b> .
S12	Fig. S7. Variable temperature NMR studies.
S13	Fig S8. Polarized optical microscopic images of compound <b>1R</b> .
S13	Fig. S9. Viscoelastic properties of <b>2R</b> .
S14	Relative quantum yield calculations of CNDs.
S14	Table S2. Quantum yield values of different CNDs
S14	Fig. S10. FT-IR spectra of purified CNDs.
S15	Fig. S11. XPS spectra of green emitting CNDs.
S16	Fig S12. XPS spectra of red emitting CNDs.

## Supporting Information

---

S16	Table S3. Composition of different elements present in green and red CNDs.
S17	Fig. S13. Lifetime plots of pure CNDs, and CNDs in gels.
S17	Table S4. Lifetime data of purified CNDs and those incorporated in gels.
S18	Fig. S14: SEM image of CNDs encapsulated MA-based chiral organogels.
S18	Fig S15. Viscoelastic properties of gels after incorporation of CNDs.
S19	Table S5. $g_{lum}$ values from the nanocomposite composed of <b>1R</b> and <b>1S</b> .
S19	Fig. S16. CPL spectra collected from multiple points on the nanocomposites.
S20	Fig. S17. CPL and fluorescence spectra of pure CNDs.
S20	Fig. S18. CPL plots for self-assembly and co-assembly experiments.
S21	Fig. S19. Excitation dependent luminescence spectra of CNDs.
S21	Fig. S20. Excitation dependent CPL spectra of the nanohybrid system.
S22	Fig. S21. CPL plots on interaction of CND with monomeric form of <b>1</b> .
S22	References

---

## Supporting Information

### 1. Experimental Section

#### 1.1 Materials

L and D-mandelic acid (MA), 1,12-diaminododecane, 1,6-diaminohexane and N,N-diisopropylethylamine (ca. 10% in N,N-dimethylformamide) were purchased from TCI India. 1-Ethyl-3-(3-dimethylaminopropyl)carbodiimide (EDC) and hydroxybenzotriazole (HOBT) were brought from Spectrochem, India. Citric acid was obtained from Merck. Ethylene diamine (EDA), urea, formamide, and anhydrous dichloromethane (DCM) were purchased from SRL. Anhydrous dimethyl sulfoxide (DMSO), anhydrous dimethyl formamide (DMF) and N-hydroxysuccinamide (NHS) were obtained from Sigma Aldrich. All reagents and chemicals were used as received without any further purification. Milli Q water was used for all the experiments.

#### 1.2 Synthesis

##### 1.2.1 Synthesis of (*R,R'*)-N,N'-(dodecane-1,12-diyl)bis(2-hydroxy-2-phenylacetamide) (**1R**)

D-Mandelic acid (1.9g, 12.5mmol) and 1, 12-diaminododecane (1.0g, 5 mmol) were added to a 250 mL round bottom flask and anhydrous DCM (60 mL) was added to it. The reaction mixture was stirred at room temperature for 30 min and then placed on ice to reduce the temperature to 0 °C. N,N-Diisopropylethylamine (3 mL) was added to the reaction mixture at 0 °C. Following this, hydroxybenzotriazole (2.1g, 14 mmol) and 1-ethyl-3-(3-dimethylaminopropyl)carbodiimide (2.7 g, 14 mmol) were added during continuous stirring. The reaction mixture was kept for stirring at room temperature for 18 h. The reaction was monitored using TLC. After the completion of reaction, purification of product was carried out by washing with 1 N HCl and brine solutions followed by extraction in DCM to obtain the product N,N'-(dodecane-1,12-diyl)bis(2-hydroxy-2-phenylacetamide) in 64.35% yield. Synthesis of the opposite isomer (**1S**) was carried out following the same procedure as above by replacing D-MA with L-MA.

<sup>1</sup>H NMR data for N,N'-(dodecane-1,12-diyl)bis(2-hydroxy-2-phenylacetamide) (500 MHz, DMSO-*d*<sub>6</sub>) δ 7.95 (t, J = 5.9 Hz, 2H), 7.41 – 7.23 (m, 10H), 6.10 (d, J = 4.7 Hz, 2H), 4.88 (d, J = 4.7 Hz, 2H), 3.05 (q, J = 6.9 Hz, 4H), 1.42 – 1.16 (m, 20H).

δ<sub>c</sub> (101 MHz, DMSO) 171.95, 141.53, 127.91, 127.33, 126.55, 73.56, 38.20, 29.15, 29.04, 29.01, 28.77, 26.31.

HRMS (m/z) calculated for C<sub>28</sub>H<sub>40</sub>N<sub>2</sub>O<sub>4</sub>, 468.3, found 491.29 [C<sub>28</sub>H<sub>40</sub>N<sub>2</sub>O<sub>4</sub>Na<sup>+</sup>].

## Supporting Information

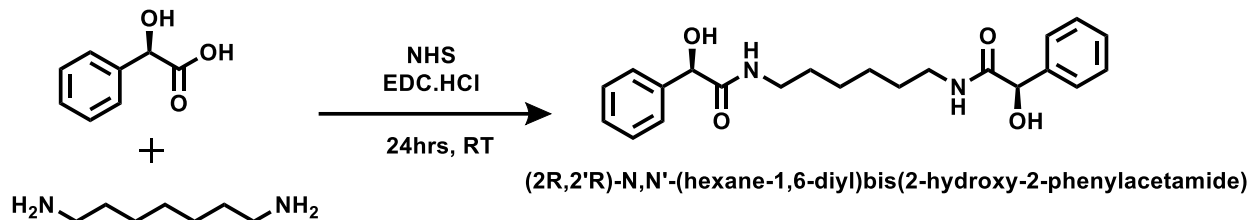


**Figure S1.** Scheme illustrating the synthesis of compound **2R**.

### 1.2.2 Synthesis of (2R,2'R)-N,N'-(hexane-1,6-diyl)bis(2-hydroxy-2-phenylacetamide) (**2R**)

L-Mandelic acid (1.06 g, 7 mmol) was dissolved in 20 mL dry THF and kept it for stirring under room temperature for 30 min. The solution was then cooled to 0-5 °C after which 7 mmol of N-hydroxysuccinamide (NHS) and EDC-HCl (7 mmol) was added and the solution was stirred for 30 min under cold conditions. The stirring was further continued for 2 h under ambient conditions. Following this, 3 mmol of 1,6-diaminohexane in 10 mL dry THF was injected to the reaction mixture upon cooling it to 0-5°C and allowed it to stir for 30 min. The reaction mixture was kept for stirring at room temperature for 24 h and was monitored using TLC. After the completion of reaction, purification of product was carried out by washing the reaction mixture with 1 N HCl and brine solutions followed by extraction in DCM to obtain (2R,2'R)-N,N'-(hexane-1,6-diyl)bis(2-hydroxy-2-phenylacetamide) in 64% yield. Synthesis of the opposite isomer (**2S**) was carried out following the same procedure as above by replacing D-MA with L-MA.

<sup>1</sup>H NMR data for (2R,2'R)-N,N'-(hexane-1,6-diyl)bis(2-hydroxy-2-phenylacetamide) (500 MHz, DMSO-*d*<sub>6</sub>) δ 7.95 (t, *J* = 5.9 Hz, 2H), 7.42 – 7.37 (m, 4H), 7.34 – 7.28 (m, 4H), 7.27 – 7.22 (m, 2H), 6.10 (d, *J* = 4.7 Hz, 2H), 4.87 (d, *J* = 4.7 Hz, 2H), 3.02 (q, *J* = 6.7 Hz, 4H), 1.34 (q, *J* = 7.0 Hz, 4H), 1.19 – 1.12 (m, 4H).

HRMS (*m/z*) calculated for C<sub>22</sub>H<sub>28</sub>N<sub>2</sub>O<sub>4</sub>, 384.2, found 407.2 [C<sub>22</sub>H<sub>28</sub>N<sub>2</sub>O<sub>4</sub>Na<sup>+</sup>].

### 1.2.3 Preparation of MA-based organogels

A typical procedure for self-assembled gel formation in DMSO/DMF-H<sub>2</sub>O binary solvent mixture is as follows: 4 mg of **1R** (or **1S**) was dissolved in 80 μL of DMSO/DMF. To this

## Supporting Information

solution, 20  $\mu\text{L}$  of  $\text{H}_2\text{O}$  was added to facilitate the gel formation. The formed product was coated onto a glass slide for further photophysical characterizations.

### 1.2.4 Synthesis and purification of CNDs

#### 1.2.4.1 Synthesis and purification of blue emitting achiral CNDs

For the synthesis of blue emitting CNDs, 1 g citric acid was dissolved in 6 mL anhydrous DMSO by stirring at room temperature. The reaction mixture was then transferred into a 50 mL Teflon-lined autoclave, sealed tightly and heated at 180  $^\circ\text{C}$  for 1.5 h. After the reaction, the hydrothermal reactor was cooled to room temperature. The as prepared CNDs were initially centrifuged at 10000 rpm for 30 min followed to remove any large particles present. The sample was subjected to dialysis against deionized water using a dialysis membrane of pore size 2.4 nm for a period of 24 h. The purified CNDs were stored in dark for further characterization.

#### 1.2.4.2 Synthesis and purification of green emitting achiral CNDs

The synthesis of green emitting CNDs was carried out using a reported procedure.<sup>1</sup> 0.192 g of citric acid along with 0.091 g of urea was dissolved in 10 mL of DMF by stirring at room temperature. The reaction mixture was then transferred into a 50 mL Teflon-lined autoclave, sealed tightly and heated at 140  $^\circ\text{C}$  for 12 h. After the reaction, the hydrothermal reactor was cooled to room temperature. The as prepared CNDs were then centrifuged at 10000 rpm for 10 min to remove any large particles present. The supernatant was collected and further purified by precipitation method. For this, 10 mL of diethyl ether was added to the CND solution followed by the dropwise addition of ethyl acetate until precipitation occurred. The precipitate was collected by centrifuging at 10000 rpm for 10 min. The obtained precipitates were then dried overnight at 60  $^\circ\text{C}$ . The purified CNDs were stored in dark.

#### 1.2.4.3 Synthesis and purification of red emitting achiral CNDs

The synthesis of red emitting CNDs was carried out using a reported procedure.<sup>2</sup> 0.6 g of citric acid along with 1.05 mL of ethylene diamine was dissolved in 40 mL of formamide by stirring at room temperature to form a transparent solution. The reaction mixture was then transferred into a 50 mL Teflon-lined autoclave, sealed tightly and heated at 180  $^\circ\text{C}$  for 4 h. After completion of reaction the hydrothermal reactor was allowed to cool down to room temperature. The as prepared CNDs were then filtered through syringe filter of 0.22  $\mu\text{m}$  pore size to remove the larger particles. To the filtered solution, 100 mL of acetone was added to form the precipitate.

## Supporting Information

The precipitate was then collected by centrifuging at 10000 rpm for 10 min. The precipitate was further washed using ethanol/acetone mixtures followed by centrifugation to obtain the purified CNDs. The obtained CNDs were dried at room temperature to remove the solvents. The purified CNDs were stored in dark.

### 1.2.5 Encapsulation of CNDs in MA-based chiral gel

A typical procedure for self-assembled gel formation in DMSO/DMF-H<sub>2</sub>O solvent mixture is as follows: 4 mg of **1R** (or **1S**) was dissolved in 80  $\mu$ L of achiral CNDs in DMSO/DMF. To this solution, 20  $\mu$ L of H<sub>2</sub>O is added to facilitate the gel formation. The obtained compound subjected to slow heating and cooling to promote proper gelation. The formed product is coated onto a glass slide for further photophysical characterizations.

### 1.3 Characterization

The fluorescence measurements were performed using JASCO-8500 fluorescence spectrophotometer. The samples for fluorescence measurements were taken in a four-sided 1 cm quartz cuvette. UV-vis characterizations were done on Agilent Cary-3500 UV-vis spectrophotometer. The samples for this were properly diluted and were taken double sided quartz cuvette. Circularly polarized luminescence (CPL) data were collected on JASCO CPL 300 spectrophotometer. The gel samples were coated on glass slides and were dried for the CPL analysis. CPL was collected from multiple spots on the slide to rule out any possibility of artefacts due to linear polarization effects. Circular dichroism (CD) data of the gel forming compound was analyzed using JASCO-1500 CD spectrometer. Morphology of the samples was investigated by using scanning electron microscope (SEM), FEI Nova Nano SEM-450 (with WDS and EDS). POM images were captured on Nikon microscope Eclipse. The samples for analysis was prepared by absorbing lyophilized samples on the carbon tapes and coated with chromium for conductivity. X-ray diffraction analysis was performed on Bruker Powder-XRD diffractometer with Ni filtered Cu-K $\alpha$  line of wavelength 0.15418 nm. <sup>1</sup>H NMR of the sample was recorded using Bruker Avance Neo 500 spectrometer (500 MHz) after dissolving the sample in *d*<sub>6</sub>-dimethylsulfoxide. The high-resolution mass data (HRMS) was collected using Orbitrap Elite HybridIon Trap-Orbitrap (ThermoFischer scientific) Mass Spectrometer.

## Supporting Information

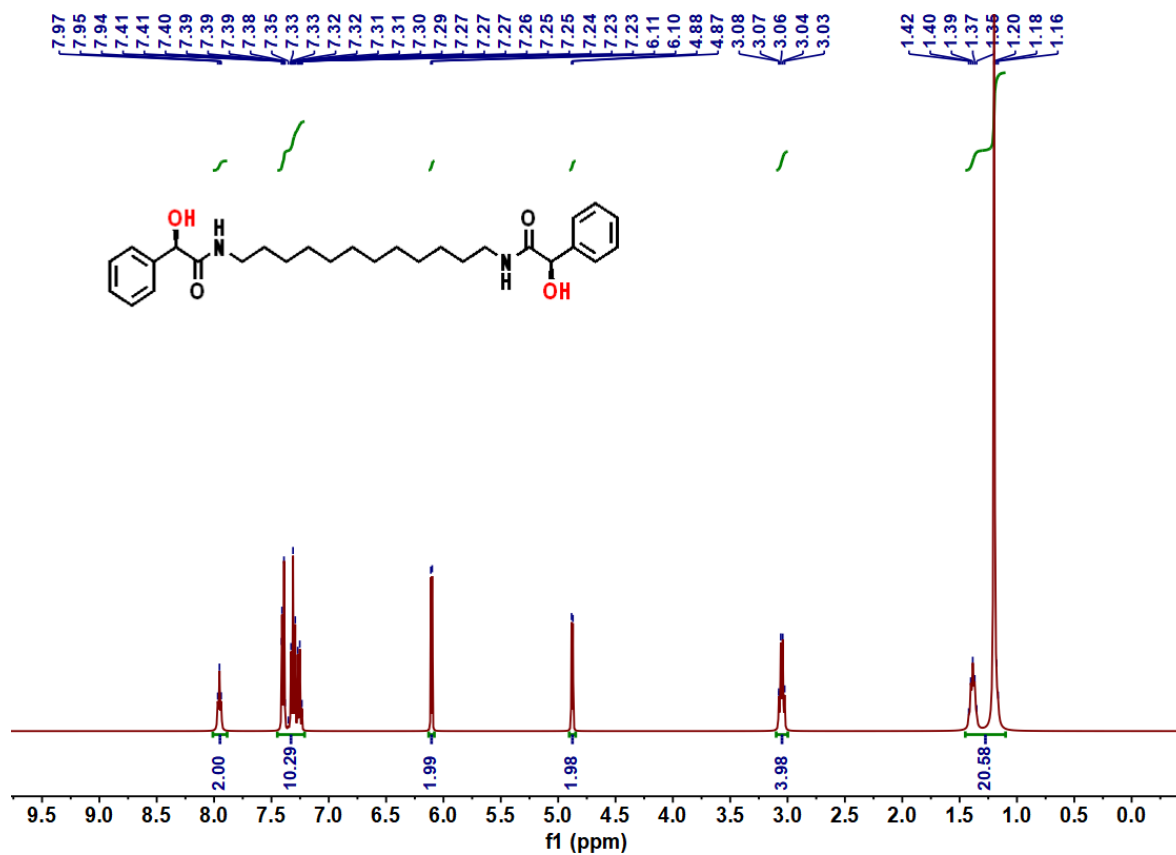
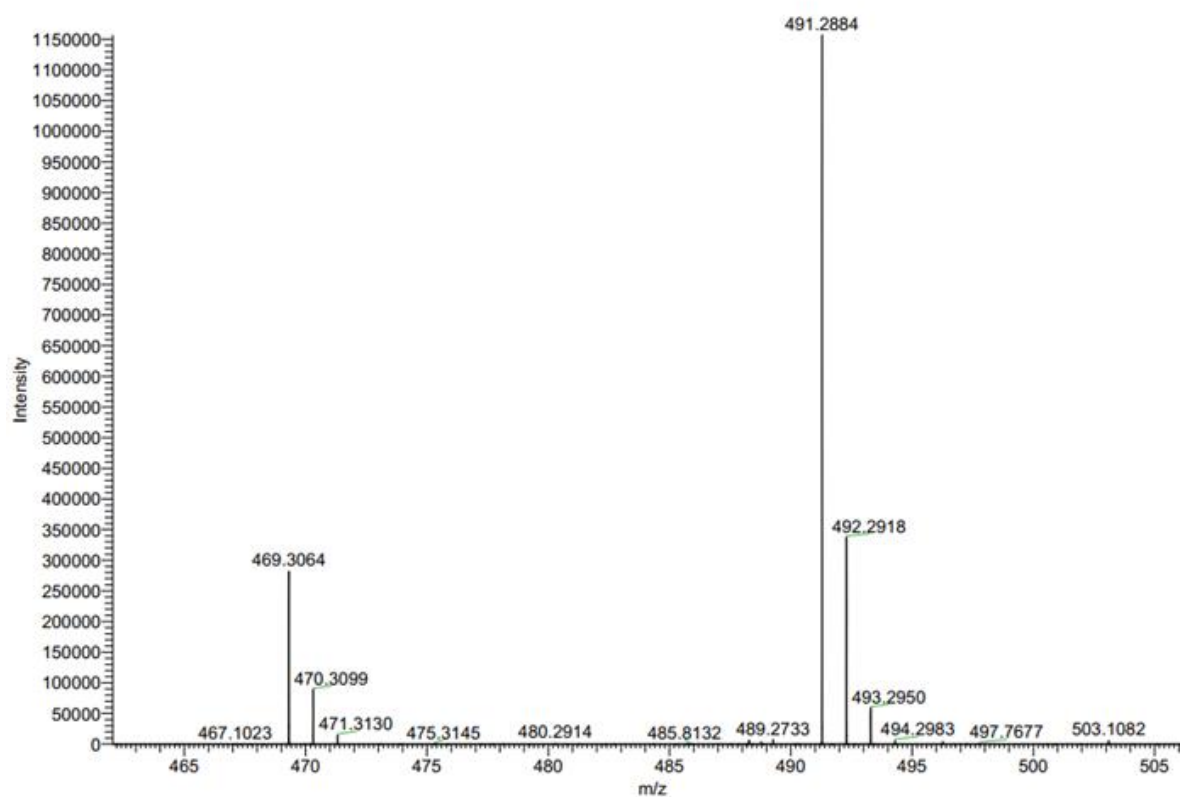


Figure S2:  $^1\text{H}$  NMR spectra of compound **1R**.





## Supporting Information



**Figure S4:** HRMS data of compound **1R**.

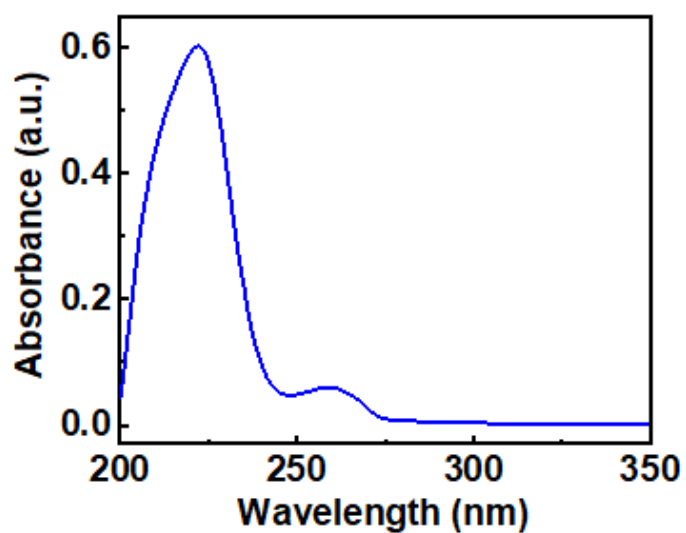


**Figure S5.** UV-visible absorption spectra of **1R** in ethanol.

## Supporting Information

**Table S1.** Behavior of **1R** in different solvent systems

<b>Solvent System</b>	<b>Result</b>
THF	Soluble
Ethanol	Soluble (upon sonication and heating)
Methanol	Soluble (upon sonication and heating)
DMF	Soluble
DMSO	Soluble
DMF:H <sub>2</sub> O (4:1)	Gel formation
DMSO:H <sub>2</sub> O (4:1)	Gel formation
THF:H <sub>2</sub> O (4:1)	Precipitate
MeOH:H <sub>2</sub> O (4:1)	Precipitate
EtOH:H <sub>2</sub> O (4:1)	Precipitate
Chloroform (CHCl <sub>3</sub> )	Insoluble
Ethyl acetate (CH <sub>3</sub> COOC <sub>2</sub> H <sub>5</sub> )	Insoluble
Acetonitrile (CH <sub>3</sub> CN)	Insoluble
Dichloromethane (DCM)	Insoluble
Hexane	Insoluble
Water (H <sub>2</sub> O)	Insoluble

Clear gelation was observed in DMF:H<sub>2</sub>O (4:1) and DMSO:H<sub>2</sub>O (4:1), and hence further investigations were carried out in these solvent compositions.

## Supporting Information

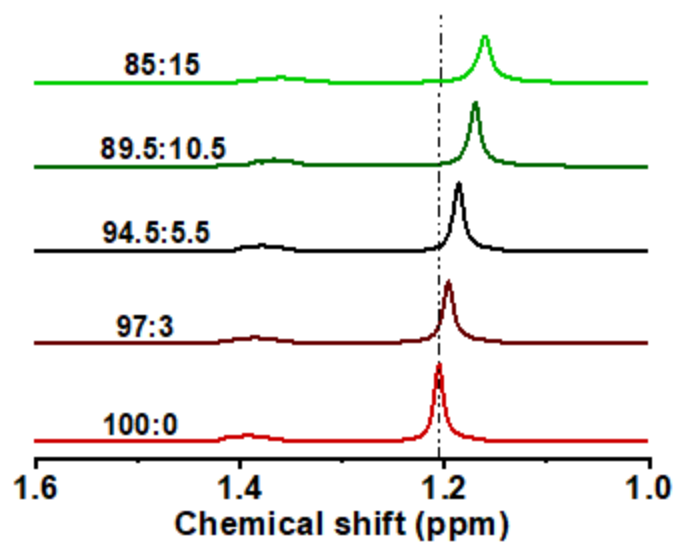


**Figure S6.** NMR spectral shifts observed in the alkyl region upon stepwise addition of D<sub>2</sub>O to compound **1** in DMSO-*d*<sub>6</sub>.

Shift in alkyl peak positions indicates the role of hydrophobic interactions between the alkyl chains during the self-assembly of the molecules in DMSO-water mixture.

## Supporting Information

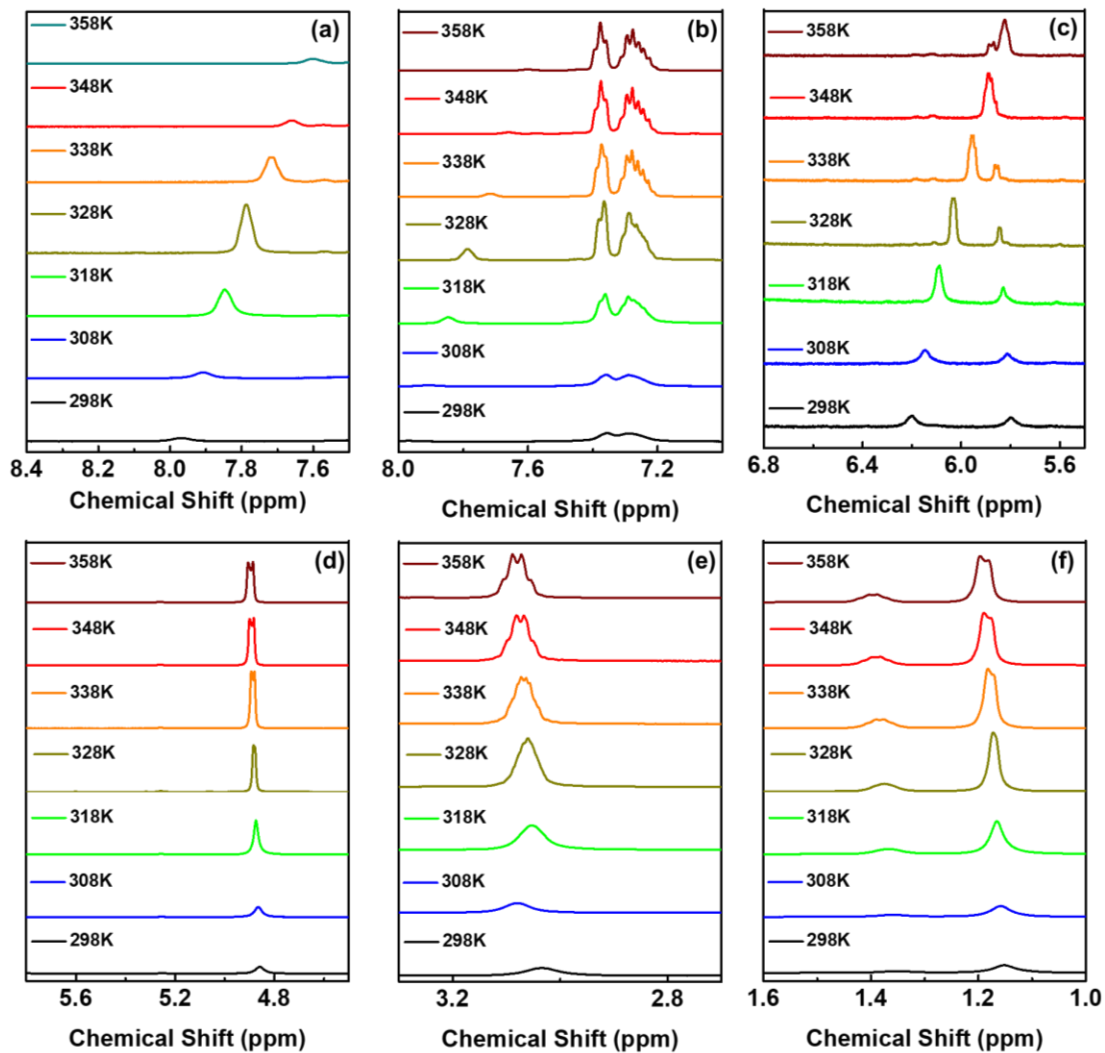


**Figure S7.** Variable temperature NMR studies of the gel formed by compound **1** in DMSO- $d_6$ /D $_2$ O mixture. The shifts corresponding to different spectral regions are shown in plots a-f.

The shifts in the peak positions are opposite to that observed in Figure 3, the titration analysis carried out to investigate the self-assembly and gelation of the compound **1**. These results emphasize the role of various noncovalent interactions in the aggregation and gelation of the compound.

## Supporting Information

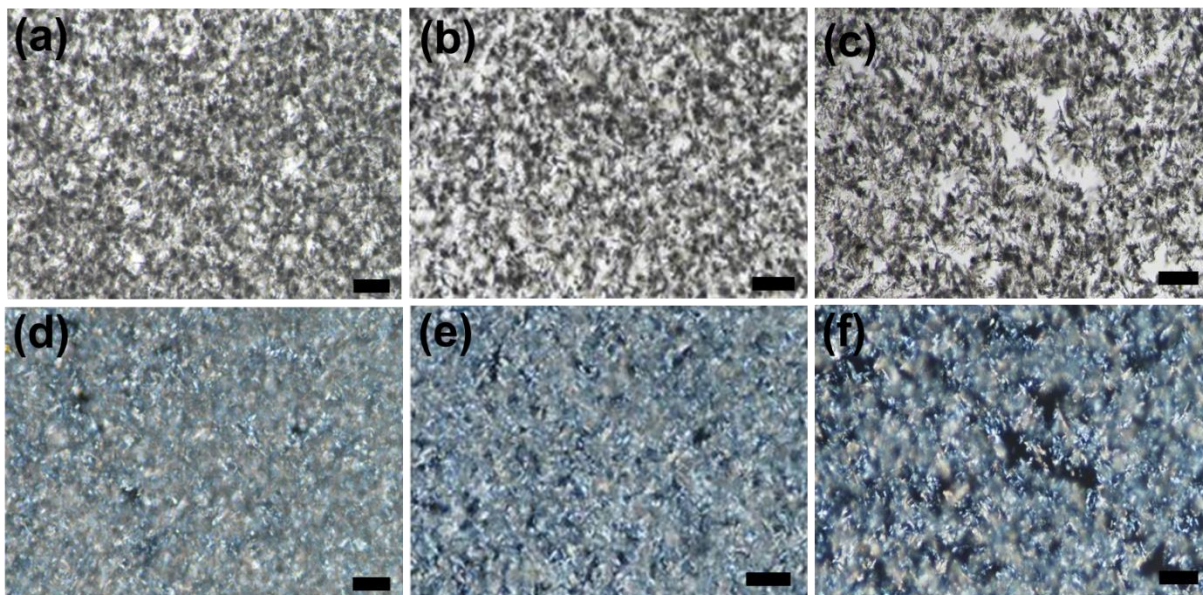


**Figure S8.** Polarized optical microscopic images of **1R** in (a,b,c) PPL and (d,e,f) (XPL crosspolarizer) configurations for (a,d) 3.2, (b,e) 4.0 and (c,f) 5.0 wt% of the gel samples (scale bar = 100  $\mu\text{m}$ ).

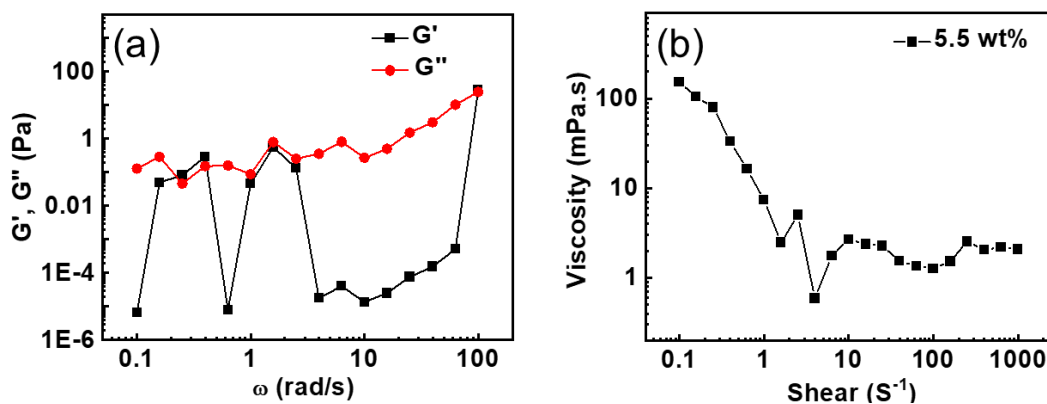


**Figure S9.** (a) Frequency sweep at  $\gamma = 1$  of gel samples from compound **2R** at varying concentrations (solid symbols and hollow symbols indicate  $G'$  and  $G''$  respectively). (b) Flow curves of gel sample of **2R** at 5.5 wt%.

## Supporting Information

### Quantum yield calculations:

The quantum yield of the as-synthesized CNDs was evaluated by adopting a relative method using quinine sulphate (in 0.1N H<sub>2</sub>SO<sub>4</sub>), Rhodamine 6G (in ethanol) and Rhodamine B (in ethanol) as reference for blue, green and red emitting CNDs respectively. The quantum yield values were calculated using the following equation:

$$\varphi_x = \varphi_{std} \left( \frac{I_x}{A_x} \right) \left( \frac{A_{std}}{I_{std}} \right) \left( \frac{\eta_x}{\eta_{std}} \right)^2$$

where  $\varphi$  denotes the luminescence quantum yield,  $I$  refer to the integrated emission intensity,  $A$  is the corresponding absorbance and  $\eta$  denotes the refractive indices of the solvent taken for the analysis. The subscript  $x$  denotes the sample whereas  $std$  refers to that of the reference compound. The calculated quantum yield values are given in the table below.

**Table S2:** Luminescence quantum yield of the purified CND samples.

CND samples	Quantum yield (%)
Blue emitting	14.3
Green emitting	9.9
Red emitting	22.2

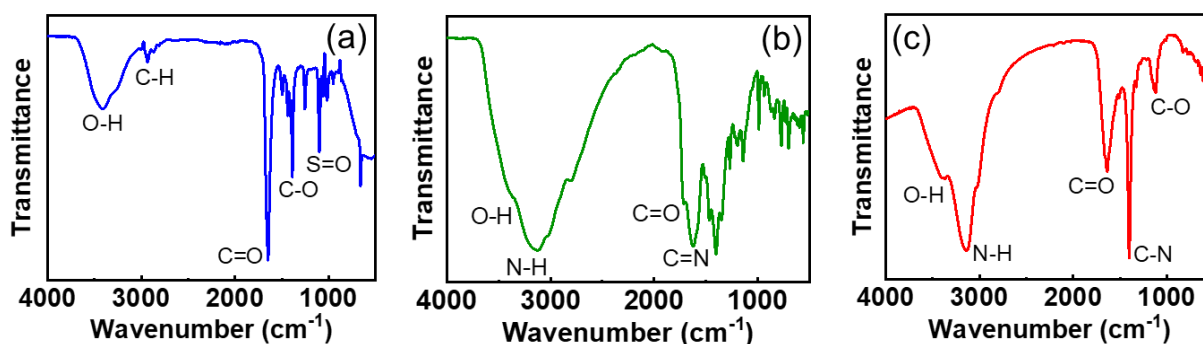


**Figure S10.** FT-IR spectra of purified (a) blue, (b) green and (c) red emitting CNDs.

## Supporting Information

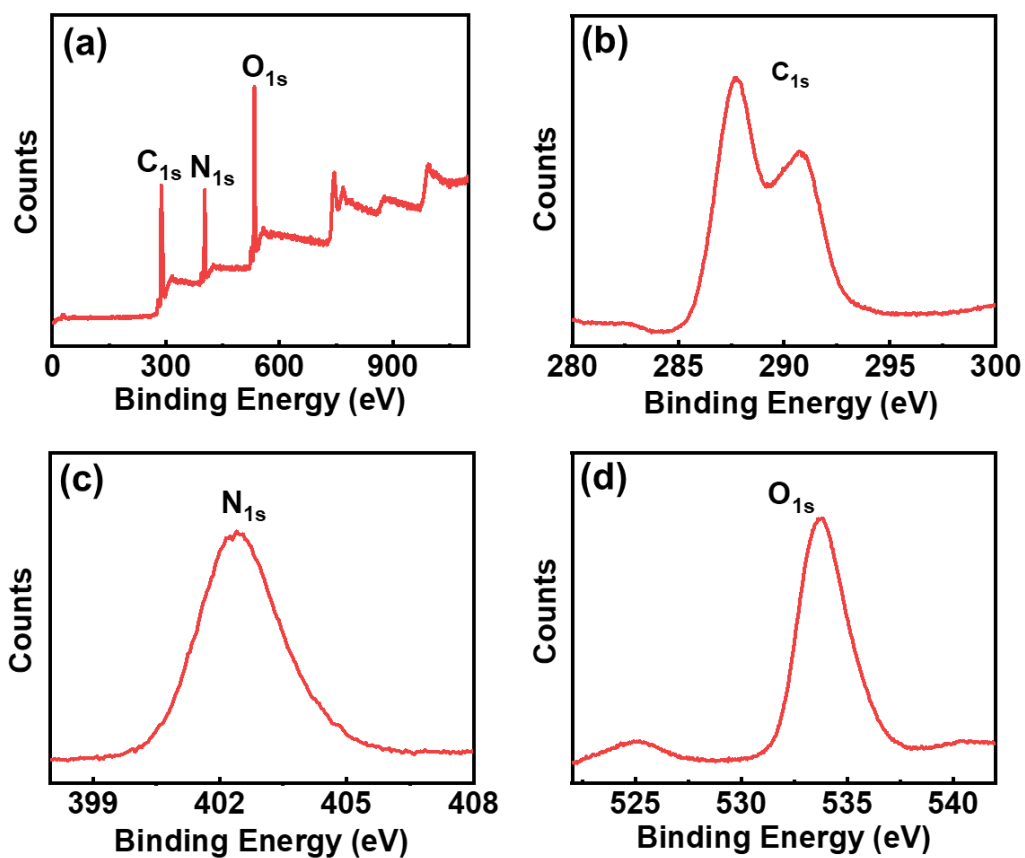


**Figure S11.** XPS spectra of green emitting CNDs: (a) survey spectrum, (b) C-1s, (c) N-1s and (d) O-1s.

## Supporting Information

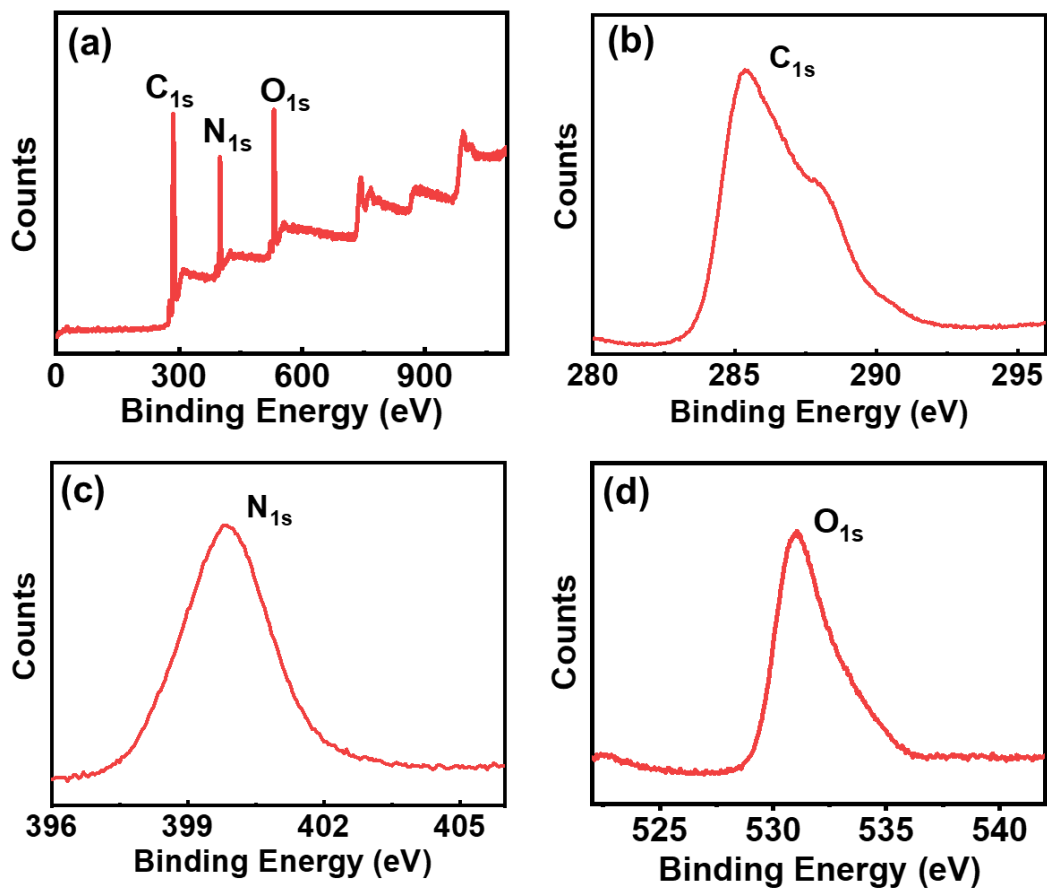


**Figure S12.** XPS spectra of red emitting CNDs: (a) survey spectrum, (b) C-1s, (c) N-1s and (d) O-1s.

**Table S3.** Composition of different elements present in green and red CNDs.

Sample	C (%)	N (%)	O (%)
Green CNDs	50.7	24.5	24.8
Red CNDs	52.4	27.8	19.8



## Supporting Information

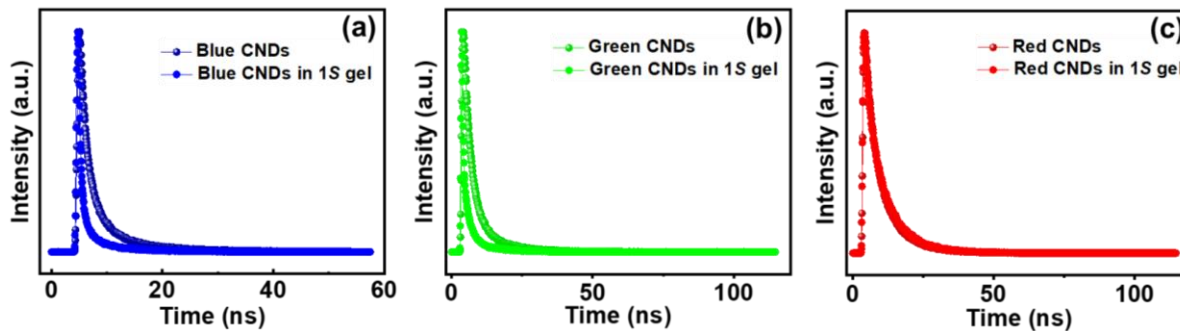


**Figure S13.** Lifetime plots for pure CNDs and the CNDs incorporated inside the gels for (a) blue, (b) green and (c) red emitting CNDs.

**Table S4.** Lifetime data of pure CNDs and the CNDs incorporated inside the gels.

	Pure CND	$\alpha$	$\chi^2$	CND-gel nanocomposite	$\alpha$	$\chi^2$
Blue emitting	$\tau_1 = 2.3$ ns	0.33	1.01	$\tau_1 = 5.0$ ns	0.38	1.09
	$\tau_2 = 8.5$ ns	0.07		$\tau_2 = 9.8$ ns	0.28	
	$\tau_3 = 0.7$ ns	0.60		$\tau_3 = 0.7$ ns	0.34	
Green emitting	$\tau_1 = 6.3$ ns	0.13	1.09	$\tau_1 = 0.2$ ns	0.85	1.14
	$\tau_2 = 2.3$ ns	0.81		$\tau_2 = 2.3$ ns	0.14	
	$\tau_3 = 13.4$ ns	0.05		$\tau_3 = 10.8$ ns	0.02	
Red emitting	$\tau_1 = 3.4$ ns	0.72	1.20	$\tau_1 = 5.0$ ns	0.46	1.09
	$\tau_2 = 8.1$ ns	0.27		$\tau_2 = 0.5$ ns	0.20	
	$\tau_3 = 10.0$ $\mu$ s	0.01		$\tau_3 = 10.8$ ns	0.34	

## Supporting Information

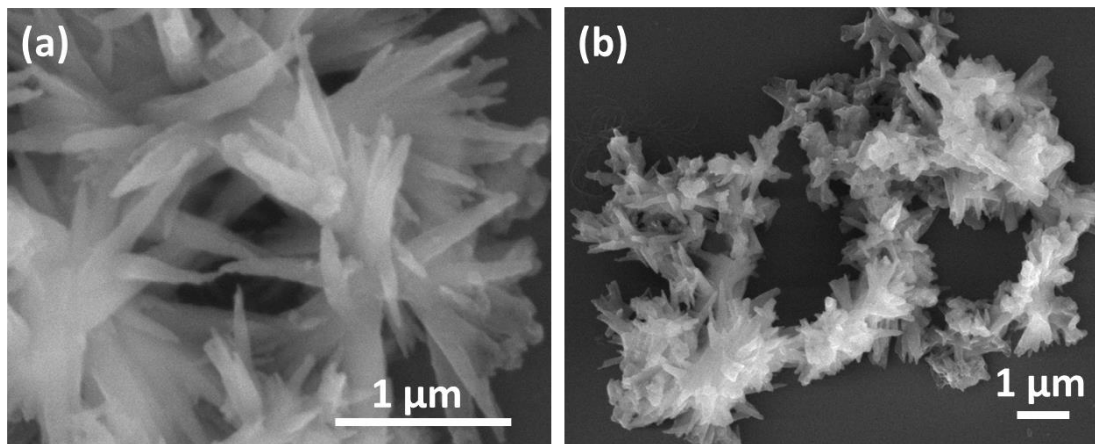


**Figure S14.** FE-SEM images of organogels formed from (a) **1S** and (b) **1R** after the encapsulation of CNDs.

No noticeable changes were observed in the structures indicating that encapsulation of CNDs does not affect the morphology of the nanostructures.

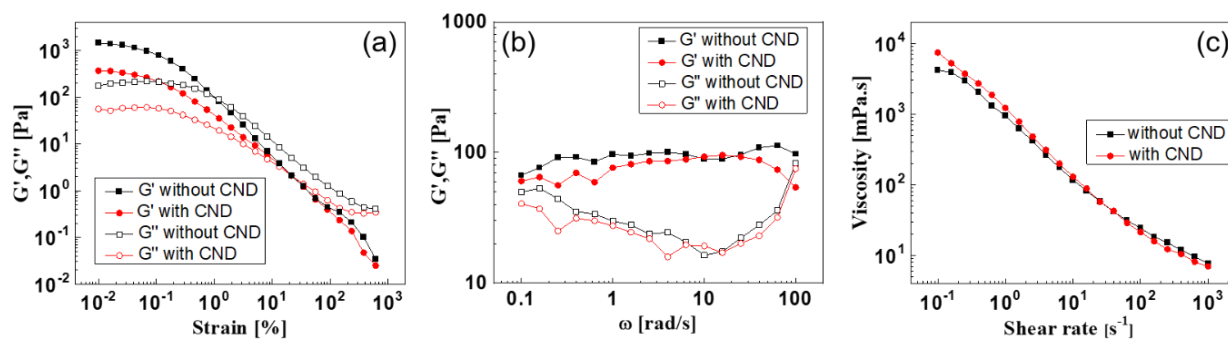


**Figure S15.** (a) Amplitude sweep at a fixed  $\omega = 10$  rad/s and (b) frequency sweep at  $\gamma = 1$  of gel samples at varying concentrations in the absence (black traces) and presence (red traces) of CNDs (solid symbols and hollow symbols indicate  $G'$  and  $G''$  respectively). (c) Flow curves of gel samples of 1R at 4.0 wt% in the absence (black traces) and presence (red traces) of CNDs.

The plots exhibit similar behavior with and without CNDs indicating that the viscoelastic properties of the gels are retained even after the incorporation of the CNDs.

## Supporting Information

**Table S5:**  $g_{lum}$  values from blue, green and red emitting CNDs when encapsulated in gels formed from **1S** and **1R**.

CPL wavelength	$g_{lum}$ on using gels formed from <b>1S</b>	$g_{lum}$ on using gels formed from <b>1R</b>
424 nm (blue)	$1.5 \times 10^{-3}$	$-5.7 \times 10^{-3}$
529 nm (green)	$2.5 \times 10^{-3}$	$-2.4 \times 10^{-3}$
608 nm (red)	$3.4 \times 10^{-3}$	$-4.5 \times 10^{-3}$

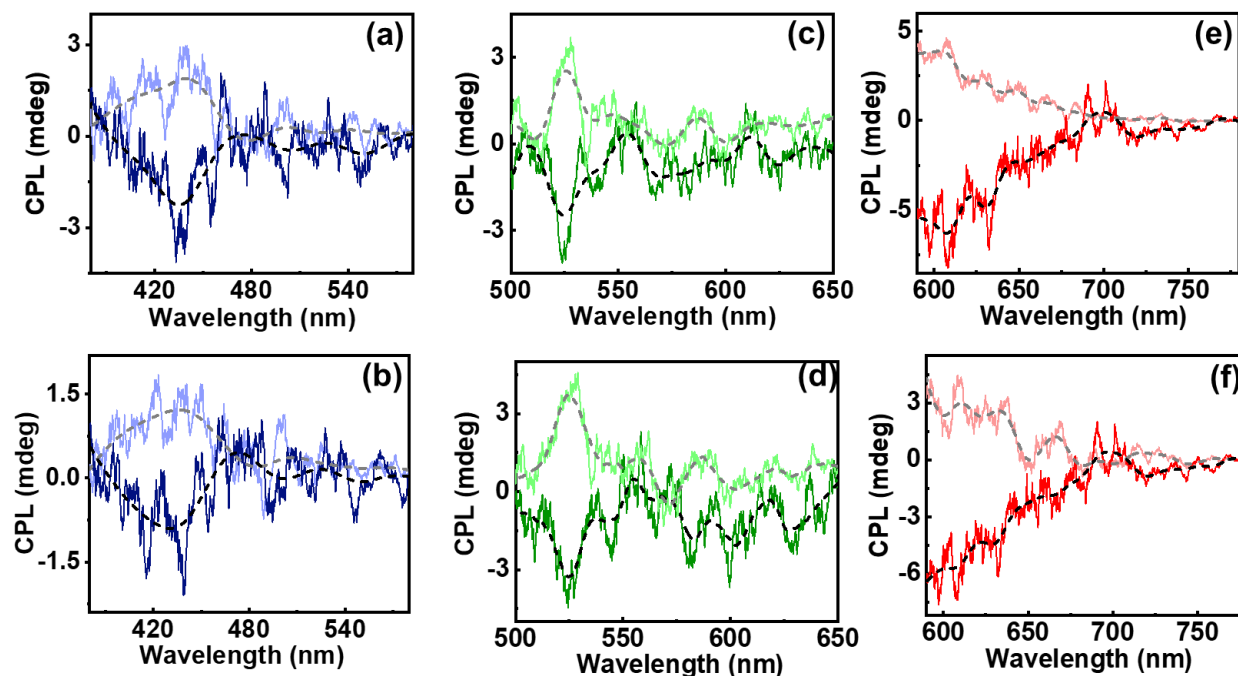


**Figure S16:** CPL spectra of the (a,b) blue, (c,d) green and (e,f) red emitting nanocomposites collected from different points on the films. Positive and negative signals correspond to the sample prepared using *R* (dark traces) and *S* (light traces) isomers of the gels.

Consistent CPL signals obtained from different points on the film confirms the reproducibility and rules out any artefacts in signals.

## Supporting Information

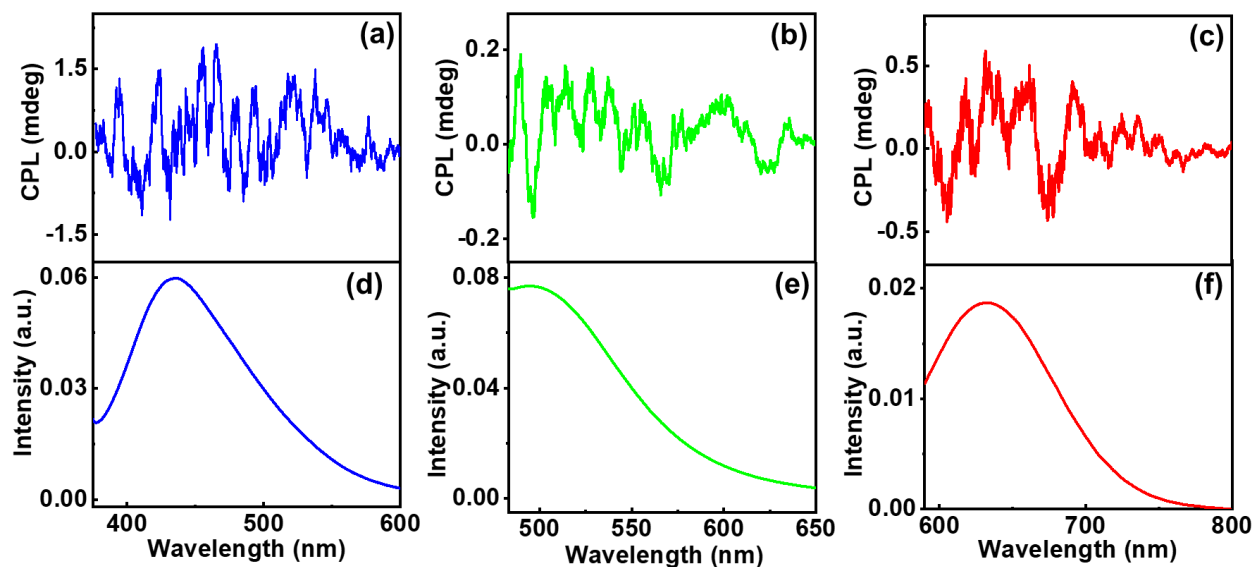


**Figure S17:** (a,b,c) CPL and (d,e,f) fluorescence spectra of (a,d) blue, (d,e) green and (c,f) red emitting achiral CNDs.

No CPL peaks were observed in any of the samples confirming that the CNDs are achiral and do not exhibit any intrinsic optical activity.

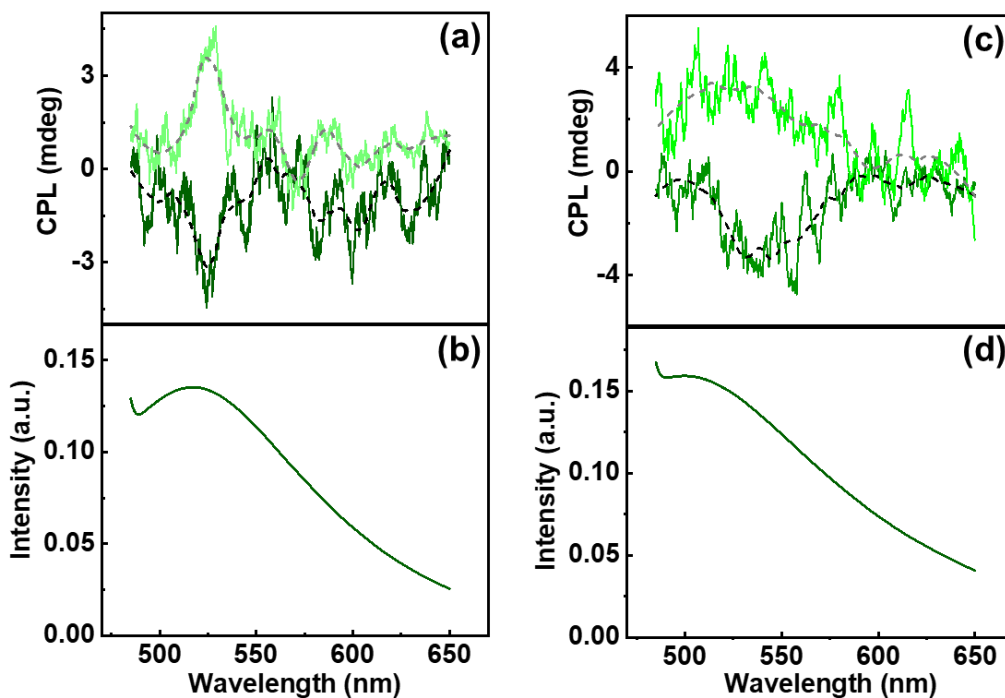


**Figure S18:** (a) CPL and (b) fluorescence signals of nanocomposites formed by the addition of DMF solution of green CNDs to powder sample of **1** (*R* and *S*), followed by stepwise addition of water. (c) CPL and (d) fluorescence signals obtained by mixing of green CND powder with preformed gels of **1** (*R* and *S*).

## Supporting Information

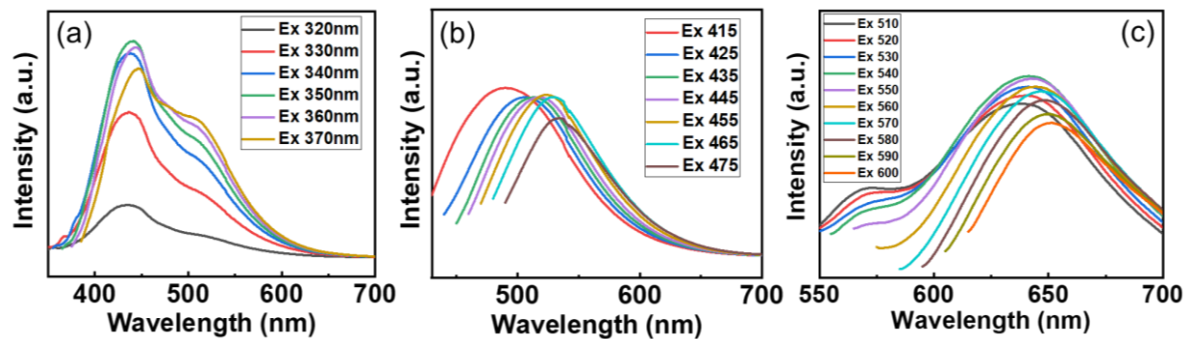


**Figure S19:** Excitation dependent luminescence spectra of (a) blue, (b) green, and (c) red emitting CNDs.

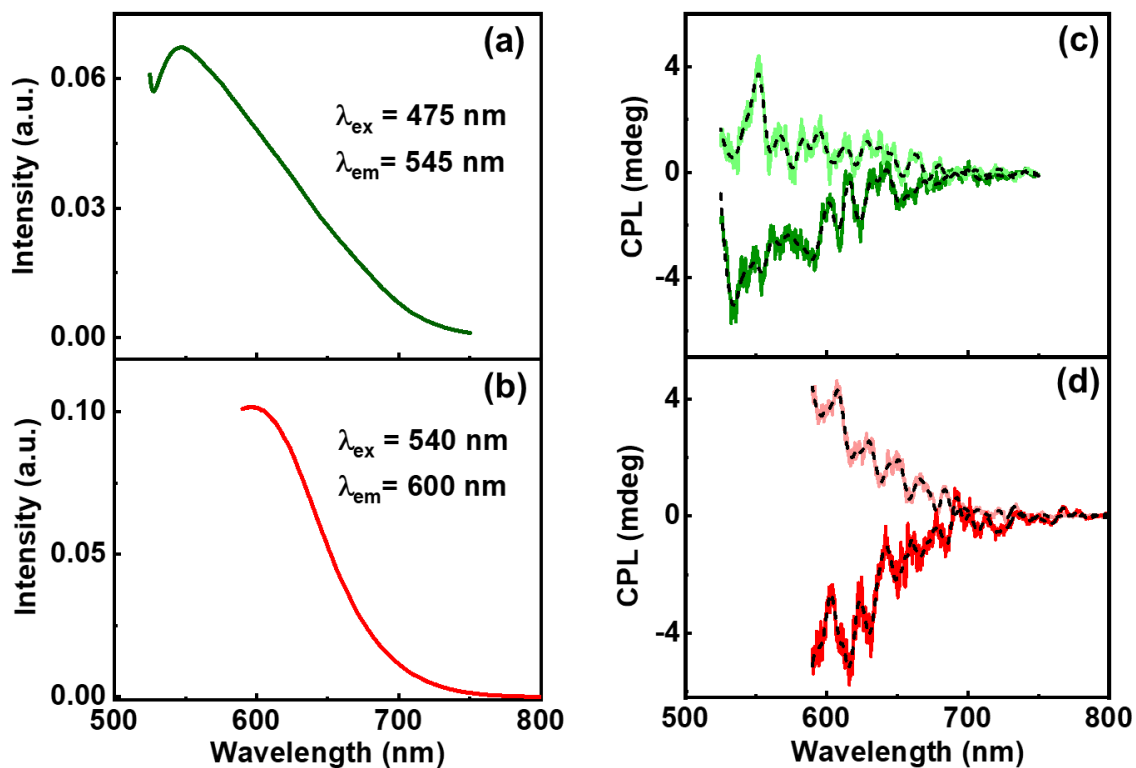


**Figure S20:** Excitation dependent (a,b) fluorescence and (c,d) CPL spectra of red emitting CNDs encapsulated in **1R** (dark traces) and **1S** (light traces). The excitation and emission wavelengths are provided in the inset.

## Supporting Information

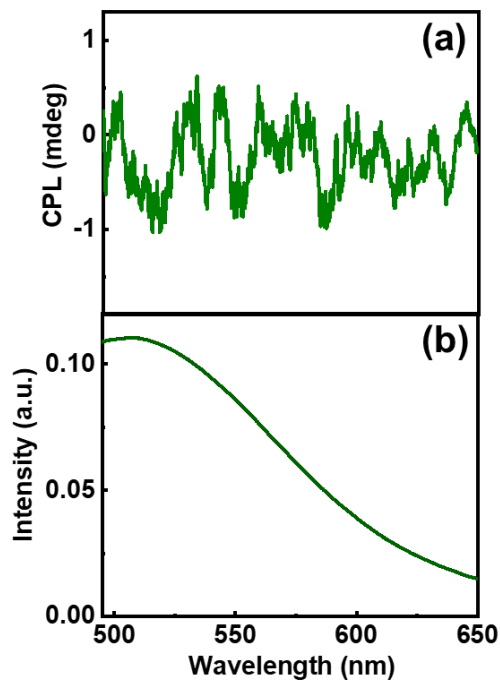


**Figure S21:** (a) CPL and (b) fluorescence plots obtained after mixing of green CNDs with **1R** in DMSO.

No CPL signals obtained for solutions in DMSO ruling out the possibility of chirality transfer from the monomeric form of the molecule to the achiral CNDs.

### References

1. X. Miao, D. Qu, D. Yang, B. Nie, Y. Zhao, H. Fan and Z. Sun, *Adv. Mater.*, 2018, **30**, 1704740.
2. H. Ding, J.-S. Wei, N. Zhong, Q.-Y. Gao and H.-M. Xiong, *Langmuir*, 2017, **33**, 12635-12642.